Supporting Information

Nickel ferrocyanides for aqueous ammonium ion batteries

Haoxiang Yu,[†,‡] Leiyu Fan,[‡] Huihui Yan,[‡] Chenchen Deng,[‡] Lei Yan,[‡] Jie Shu,[‡,] Zhen-Bo Wang,[†,**]*

[†] MIIT Key Laboratory of Critical Materials Technology for New Energy Conversion and Storage, School of Chemistry and Chemical Engineering, State Key Lab of Urban Water Resource and Environment, Harbin Institute of Technology, Harbin, Heilongjiang, 150001, China

[‡] School of Materials Science and Chemical Engineering, Ningbo University, Ningbo, Zhejiang, 315211, China

** Corresponding author: Jie Shu*

E-mail: shujie@nbu.edu.cn

*** Corresponding author: Zhen-Bo Wang*

E-mail: wangzhb@hit.edu.cn

Table of Contents

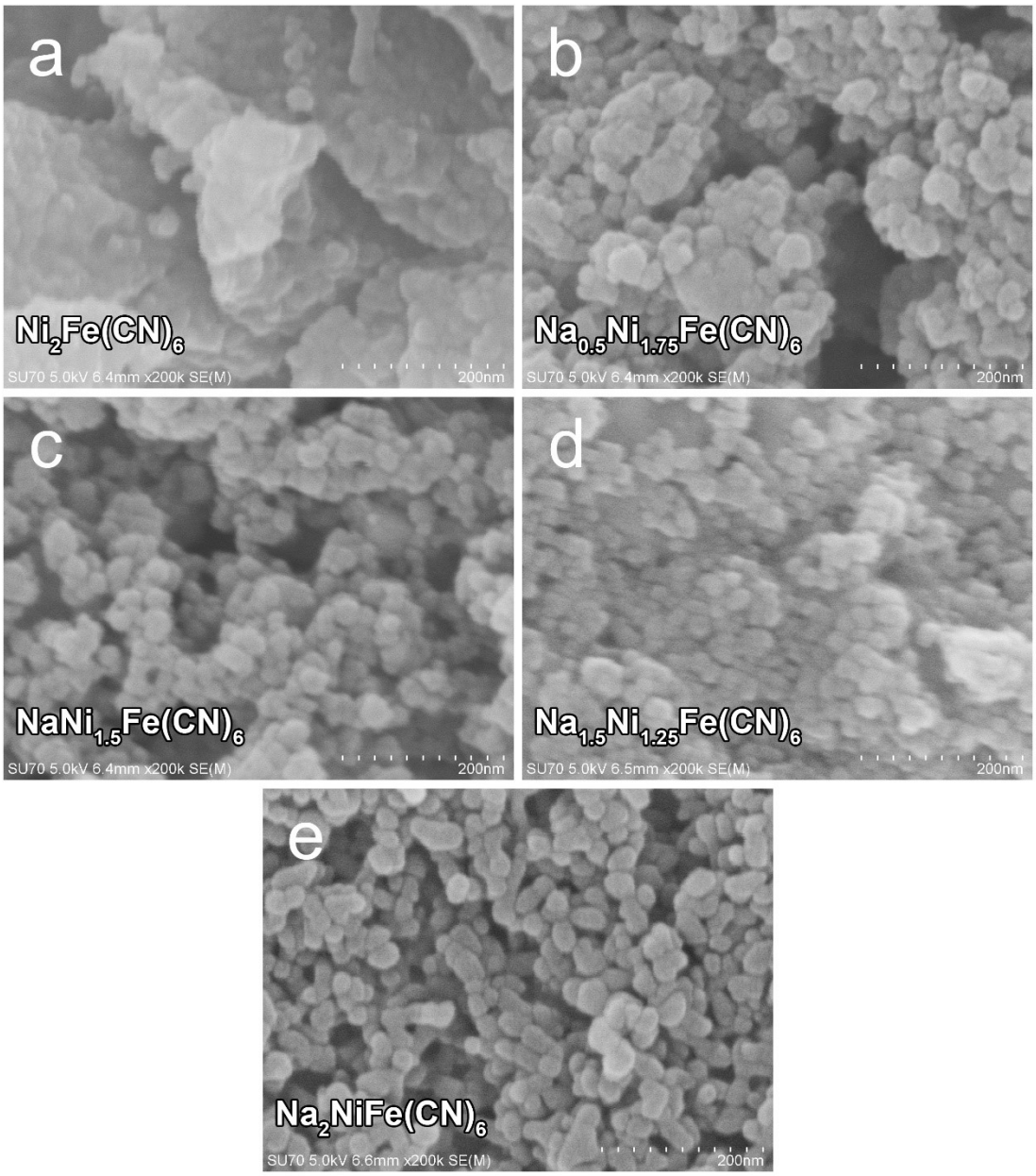

Figure S1. SEM images with large magnification of (a) $Ni_2Fe(CN)_6$; (b) $Na_{0.5}Ni_{1.75}Fe(CN)_6$; (c) $NaNi_{1.5}Fe(CN)_6$; (d) $Na_{1.5}Ni_{1.25}Fe(CN)_6$; (e) $Na_2NiFe(CN)_6$.

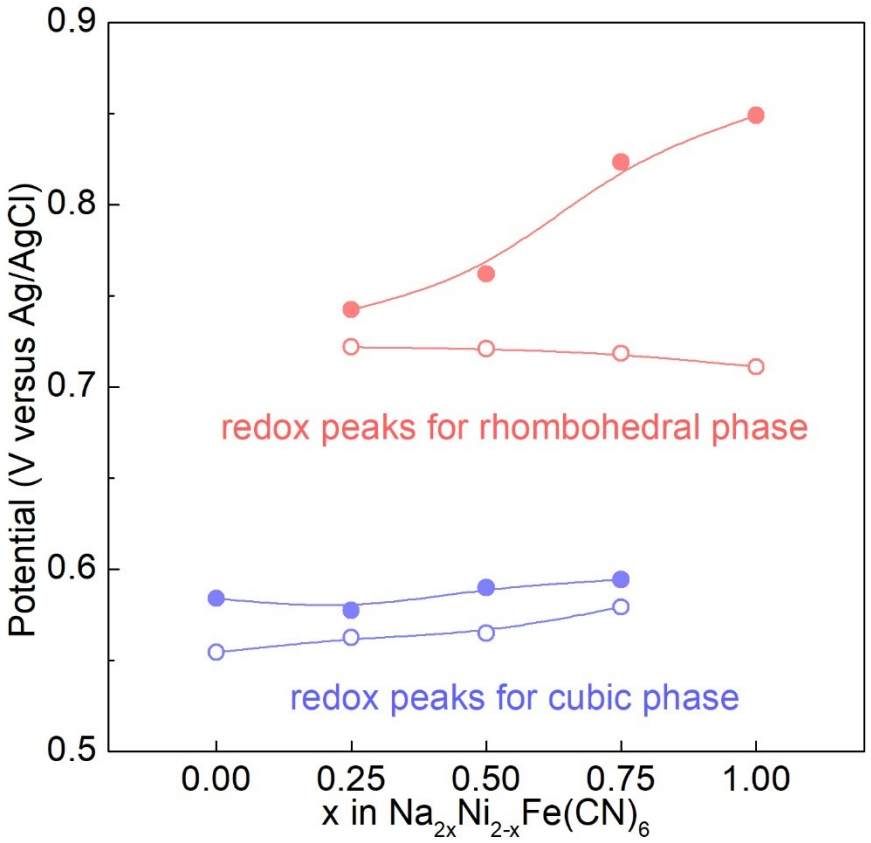

Figure S2. Graph of the redox peak plotted against x in $Na_{2x}Ni_{2-x}Fe(CN)_6$ (x = 0, 0.25, 0.5, 0.75, and 1).

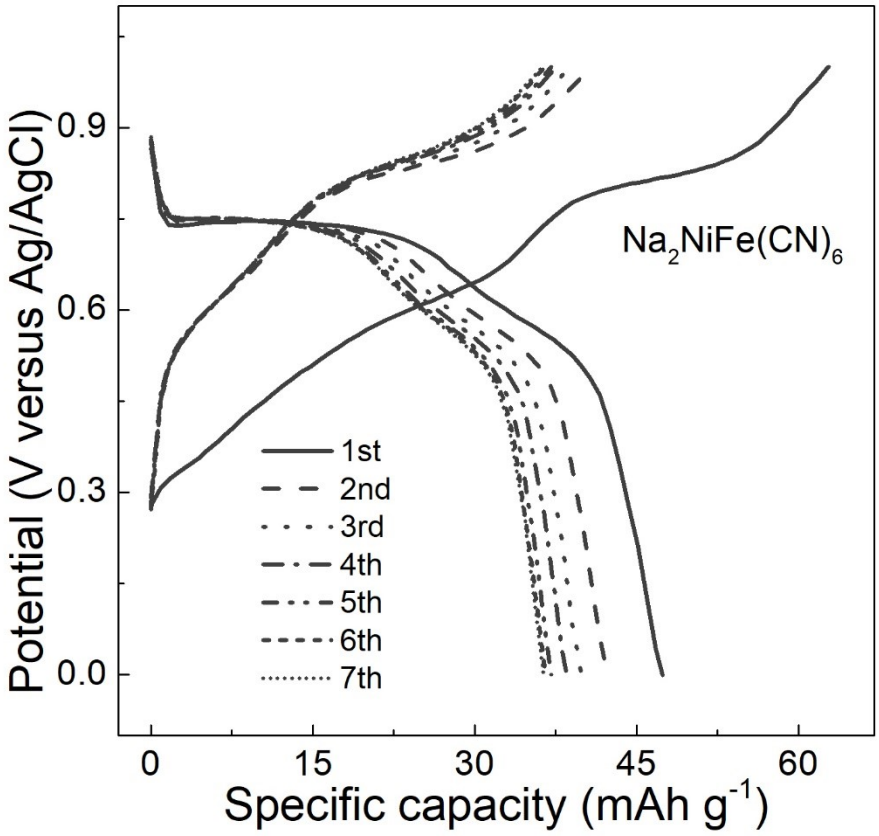

Figure S3. First seven potential curves of $Na_2NiFe(CN)_6$ at 1 C.

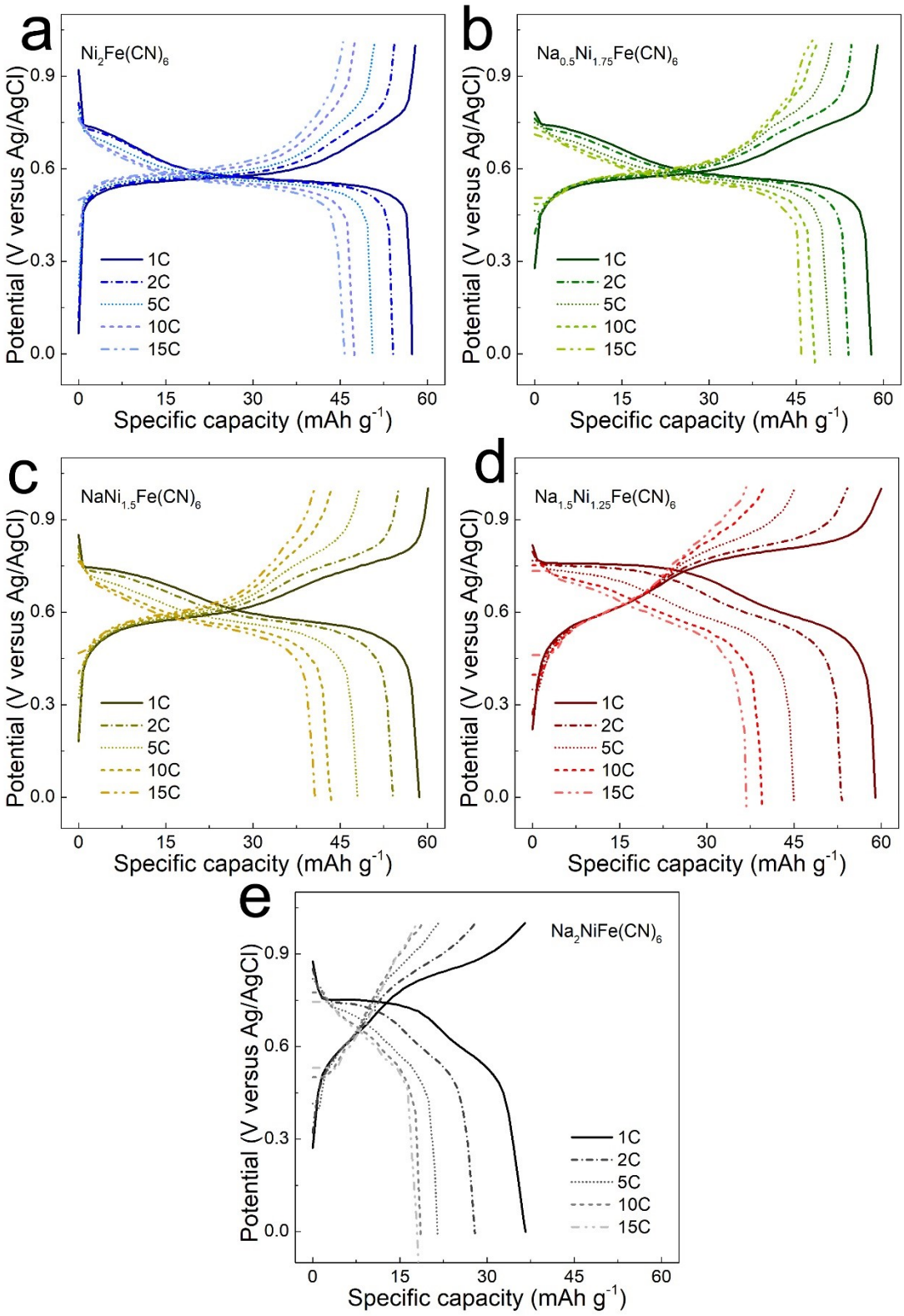

Figure S4. Galvanostatic potential profiles of (a) $Ni_2Fe(CN)_6$; (b) $Na_{0.5}Ni_{1.75}Fe(CN)_6$; (c) $NaNi_{1.5}Fe(CN)_6$; (d) $Na_{1.5}Ni_{1.25}Fe(CN)_6$; (e) $Na_2NiFe(CN)_6$ at various current rates.

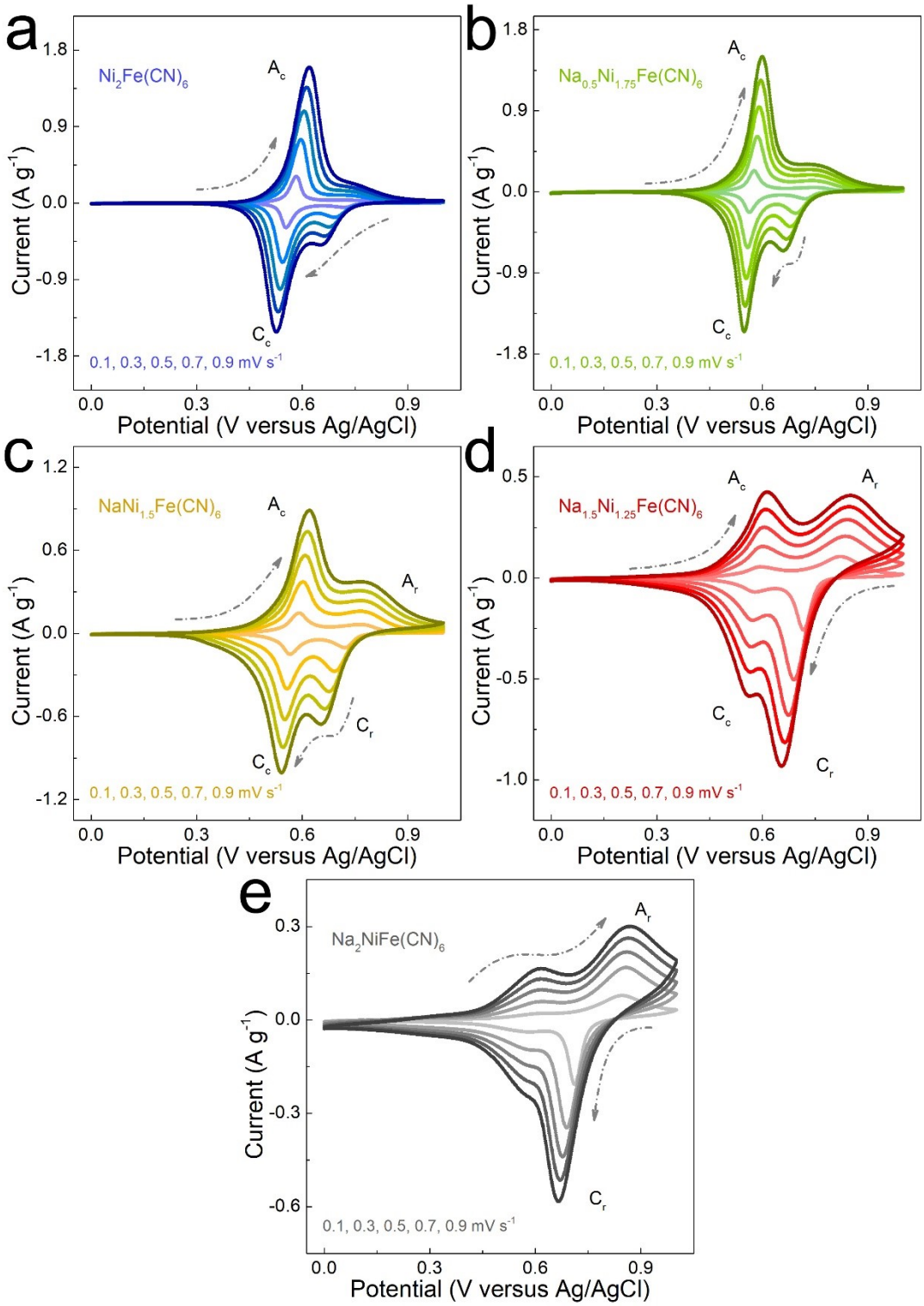

Figure S5. CV profiles of (a) $Ni_2Fe(CN)_6$; (b) $Na_{0.5}Ni_{1.75}Fe(CN)_6$; (c) $NaNi_{1.5}Fe(CN)_6$; (d) $Na_{1.5}Ni_{1.25}Fe(CN)_6$; (e) $Na_2NiFe(CN)_6$ at different scan rates.

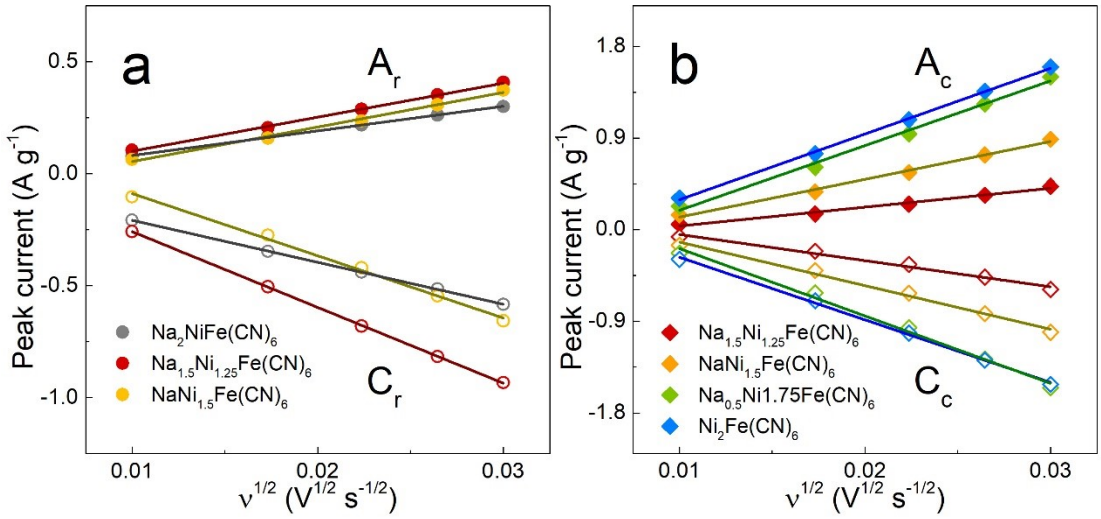

Figure S6. Linear relationship of the peak current and the square root of scan rate ($\nu^{1/2}$) for (a) rhombohedral phase and (b) cubic phase of $Na_{2x}Ni_{2-x}Fe(CN)_6$ (x = 0, 0.25, 0.5, 0.75, and 1).

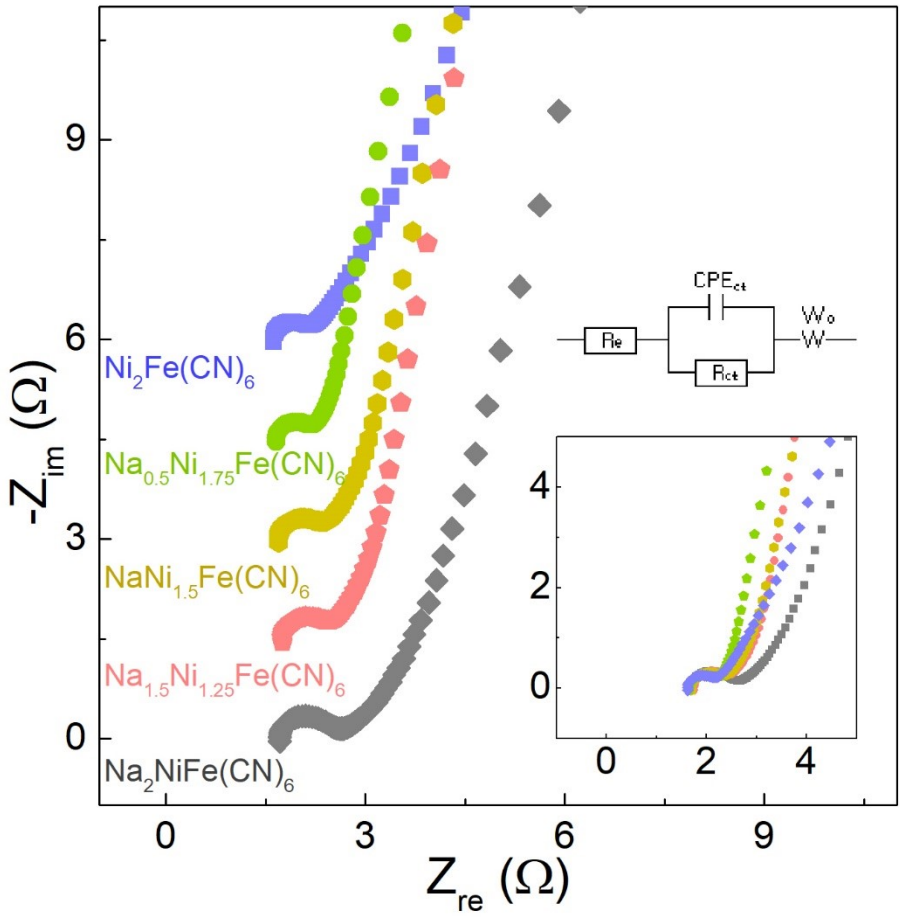

Figure S7. Nyquist plots of $Na_{2x}Ni_{2-x}Fe(CN)_6$ (x = 0, 0.25, 0.5, 0.75, and 1). The inset shows an enlargement of Nyquist plots and an equivalent circuit.

Table S1. ICP-OES analysis of $Ni_2Fe(CN)_6$, $Na_{0.5}Ni_{1.75}Fe(CN)_6$, $NaNi_{1.5}Fe(CN)_6$, $Na_{1.5}Ni_{1.25}Fe(CN)_6$, and $Na_2NiFe(CN)_6$.

	Na	**Ni**	**Fe**
$Ni_2Fe(CN)_6$	4.3549%	23.1807%	11.6106%
$Na_{0.5}Ni_{1.75}Fe(CN)_6$	5.6718%	23.6330%	13.7176%
$NaNi_{1.5}Fe(CN)_6$	6.5047%	21.0285%	13.4359%
$Na_{1.5}Ni_{1.25}Fe(CN)_6$	7.0720%	14.3564%	10.8211%
$Na_2NiFe(CN)_6$	7.6944%	11.9442%	9.9176%

Table S2. Comparison of rate capacities of $Na_{2x}Ni_{2-x}Fe(CN)_6$ (x = 0, 0.25, 0.5, 0.75, and 1).

	Capacity (mAh g^{-1})				
	1 C	**2 C**	**5 C**	**10 C**	**15 C**
$Ni_2Fe(CN)_6$	57.4	54.1	50.6	47.5	45.8
$Na_{0.5}Ni_{1.75}Fe(CN)_6$	57.9	54.0	50.9	48.2	45.9
$NaNi_{1.5}Fe(CN)_6$	58.6	54.1	48.0	43.5	40.7
$Na_{1.5}Ni_{1.25}Fe(CN)_6$	59.0	53.3	45.0	39.5	36.8
$Na_2NiFe(CN)_6$	36.6	27.9	21.5	18.6	18.2

Table S3. Diffusion coefficients calculated from CV.

	D for Rhombohedral phase ($cm^2\ s^{-1}$)		D for Cubic phase ($cm^2\ s^{-1}$)	
	A_r*	C_r*	A_c*	C_c*
$Ni_2Fe(CN)_6$	--#	--#	2.85×10^{-9}	2.58×10^{-9}
$Na_{0.5}Ni_{1.75}Fe(CN)_6$	--#	--#	2.76×10^{-9}	2.99×10^{-9}
$NaNi_{1.5}Fe(CN)_6$	1.63×10^{-10}	5.27×10^{-10}	9.42×10^{-10}	1.25×10^{-9}
$Na_{1.5}Ni_{1.25}Fe(CN)_6$	1.57×10^{-10}	7.82×10^{-10}	2.35×10^{-10}	4.52×10^{-10}
$Na_2NiFe(CN)_6$	8.25×10^{-11}	2.40×10^{-10}	--#	--#

* A_r: anodic peak current for rhombohedral phase; C_r: cathodic peak current for rhombohedral phase; A_c: anodic peak current for cubic phase; C_c: cathodic peak current for rhombohedral phase.

The values can hardly be calculated because the corresponding peak currents are difficult to identify.